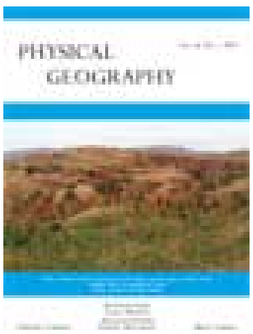

Physical Geography

ISSN: 0272-3646 (Print) 1930-0557 (Online) Journal homepage: https://www.tandfonline.com/loi/tphy20

A record of flooding on the White River, Arkansas derived from tree-ring anatomical variability and vessel width

Matthew D. Meko & Matthew D. Therrell

To cite this article: Matthew D. Meko & Matthew D. Therrell (2019): A record of flooding on the White River, Arkansas derived from tree-ring anatomical variability and vessel width, Physical Geography, DOI: 10.1080/02723646.2019.1677411

To link to this article: https://doi.org/10.1080/02723646.2019.1677411

PHYSICAL GEOGRAPHY
https://doi.org/10.1080/02723646.2019.1677411

Taylor & Francis
Taylor & Francis Group

ARTICLE

A record of flooding on the White River, Arkansas derived from tree-ring anatomical variability and vessel width

Matthew D. Meko[a] and Matthew D. Therrell[b]

[a]Laboratory of Tree-Ring Research, University of Arizona, Tucson, AZ, USA; [b]Department of Geography, University of Alabama, Tuscaloosa, AL, USA

ABSTRACT

Tree rings preserve important records of past flooding. We present the results of an examination of inter-annual tree-ring anatomical variability and vessel width in overcup oak (*Quercus lyrata*) and river flooding at a bottomland hardwood forest site near the confluence of the White and Mississippi Rivers. We developed two flood chronologies based on (1) visual identification of "flood-ring" anatomical anomalies and (2) a simple method for quantitative measurements of earlywood vessel width (VW). Using visual flood rings, we have developed a response index (RI) chronology of floods from 1780–2013 and, using the VW measurements, we have developed a quantitative reconstruction of spring river levels from 1800–2013. Both the RI and VW chronologies are strongly related to spring river flooding and indicate that major floods such as those in 1805, 1826, 1844, 1852, 1858, occurred in the period prior to the systematic collection of stage data, and that the frequency of extreme events has greatly varied over the past two centuries. These chronologies provide important new information about Lower Mississippi River flooding in past centuries, and our simple method of measuring VW is a potentially useful new approach to the development of tree-ring records of flooding.

ARTICLE HISTORY
Received 17 April 2019
Accepted 4 October 2019

KEYWORDS
Dendrochronology; dendrohydrology; tree ring; flood ring; paleoflood; White River

Introduction

River flooding routinely affects millions of people worldwide, (Jonkman, 2005). In the United States, flooding represents one of the most deadly weather related hazards and annually causes tens of millions of dollars in economic losses (Ashley & Ashley, 2008; Downton, Miller, & Pielke, 2005). These threats to life and property make floods an important topic in hydrological and atmospheric research (Changnon & Kunkel, 1995; Knox, 2000; Munoz & Dee, 2017; Pinter, Jemberie, Remo, Heine, & Ickes, 2008). Statistical models used to predict the magnitude and frequency of future floods primarily rely on instrumental and historical measurements of flood stage and discharge (Baker, 1987; England et al., 2017; Stedinger & Griffis, 2008); however, instrumental records prior to the late 19th century are rare, and lack adequate temporal and spatial resolution, hindering quantification of the potential range of severity and temporal pattern of floods (Benito et al., 2004; Brázdil, Kundzewicz, & Benito, 2006; Costa, 1987; Klemeš, 1989). Studies of paleofloods – those floods that occurred before the instrumental record – can

CONTACT Matthew D. Therrell mdtherrell@ua.edu

augment temporal and spatial coverage of current flood records and shed light on the frequency and magnitude of extreme events (Knox, 2000). In fact, new draft U.S. federal guidelines for determining flood frequency include using confidence interval formulas that account for paleoflood information (England et al., 2017). Indirect evidence of floods that occurred before the systematic hydrologic record includes sediment deposits, landforms, and vegetation (Costa, 1987).

Tree-ring width data have been widely used throughout the western U.S. to reconstruct streamflow (Coulthard, Smith, & Meko, 2016; Ho, Lall, & Cook, 2016; Meko, Therrell, Baisan, & Hughes, 2001; Woodhouse & Lukas, 2006), but tree-ring streamflow reconstructions are less common in the eastern U.S. (Cleaveland, 2000; Devineni, Lall, Pederson, & Cook, 2013; Ho, Lall, Sun, & Cook, 2017; Maxwell et al., 2017). In addition, despite providing valuable information on past drought and pluvial episodes at annual or seasonal timescales, such records are not well suited to examining seasonal flooding. This is because short-duration flood peaks are often not reflected in the response of radial tree growth to hydroclimate (Ballesteros-Cánovas, Stoffel, St George, & Hirschboeck, 2015). Tree-ring records from riparian settings can be suitable for the study of paleoflood hydrology because these trees often record evidence of past short-term streamflow variability (i.e. flooding), and that evidence can be accurately located in time using dendrochronological dating methods. For example, when trees are struck by flood-borne debris, the formation of scar tissue after local cambial death can allow the dating of past floods with annual to subannual precision and the height of scarring along the tree stem can serve as a minimum estimate of past flood stage (Ballesteros-Cánovas et al., 2015; Harrison & Reid, 1967; McCord, 1996; Sigafoos, 1964). In addition, defoliation of the crown or prolonged inundation of roots and stem can interfere with physiological processes controlling xylem formation. This can result in distinct flood-related anatomical anomalies within the annual growth increment, termed "flood rings," that mark the year and possibly the season of flood occurrence (Astrade and Bégin, 1997; Copini et al., 2016; Kames, Tardif, & Bergeron, 2016; St. George & Nielsen, 2000; Tardif, Kames, & Bergeron, 2010; Therrell & Bialecki, 2015; Yanosky, 1983).

Under normal growing conditions, ring-porous trees such as *Quercus* spp. form distinct earlywood (EW) tissue characterized by single or multiple ranks of large conductive vessels formed during leaf expansion and twig elongation in spring; latewood (LW) tissue exhibits much smaller vessels and is characterized by dense fiber and flame parenchyma cells (St. George, 2010; Yanosky & Jarrett, 2002). Inundation of roots and stem of ring-porous tree species can lead to a variety of abnormalities in annual ring tissues. Yanosky (1983, 1984)) found that *Fraxinus* spp. that experienced defoliation during summer floods developed LW tissues that exhibited some characteristics of EW, such as enlarged vessels and abnormally thin fiber-cell walls. Astrade and Bégin (1997) found that *Q. robur* trees developed abnormally small and disorganized EW vessels in response to root inundation during spring flooding. St. George and Nielsen (2003) used *Q. macrocarpa* flood rings exhibiting similar anatomical anomalies to construct a proxy record of extreme floods in the lower Red River, Manitoba.

At present, most paleoflood chronologies developed from anatomical anomalies within tree rings of ring-porous species primarily rely on visual identification of flood rings, resulting in categorical presence/absence data (St. George & Nielsen, 2003; Therrell & Bialecki, 2015; Wertz, St. George, & Zeleznik, 2013). However, such measurements (e.g. mean vessel area)

can contain environmental information not present in the signal of other tree-ring metrics such as ring width (Fonti & García-González, 2004). For example, Woodcock (1989) developed a reconstruction of October-June precipitation using *Q. macrocarpa* latewood vessel diameter. García-González and Eckstein (2003) determined that vessel lumen areas of *Q. robur* reflected March and April temperature and precipitation. García-González and Fonti (2006) found that chronologies of *Castanea sativa* vessel area incorporating different size classes of vessels contained different signals, and that vessel area chronologies incorporating all sizes of vessels yielded weaker climate-growth relationships. Fonti, Solomonoff, and García-González (2007) found *C. sativa* mean vessel area chronologies contained both a negative February-March temperature signal, and a positive April temperature signal. Fonti and García-González (2008) found that mean vessel area had a different and stronger response to climate compared to that of ring-width variables, especially at mesic sites, where mean vessel area correlated strongly with spring precipitation.

These types of measurements may also contain information about magnitude and duration of flood events that occurred during cell formation. For example, Astrade and Bégin (1997) determined that a marked reduction in mean and standard deviation of EW vessel lumen area in *Q. robur* trees growing in floodplain forests of the Saone River, France, was caused by severe late spring flooding on the Saone. St. George, Nielsen, Conciatori, and Tardif (2002) found that *Q. macrocarpa* rings with EW vessel areas roughly two standard deviations below the mean coincided with major floods, but these measurements did not produce information that was not already evident through visual inspection under the microscope. Nonetheless, that study concluded that vessel area series were useful for the reconstruction of extreme flood frequency. López, Del Valle, and Giraldo (2014) reconstructed water levels of the Atrato River in the Darien Gap in Panama from a chronology based upon the number of vessels in the annual growth ring of the tropical floodplain-forest tree *Prioria copaifera*. More recently, Kames et al. (2016) developed continuous earlywood vessel chronologies responsive to streamflow and flooding in Quebec.

In this study we present two records of flooding near the confluence of the White and Mississippi Rivers based on a conventional visual record of "flood rings" as well as EW vessel width. To assess the applicability of these records as flood indicators, we compare them to climate and river stage data and discuss the strengths and weaknesses of our new records with respect to potential contribution to the paleoflood record in the region.

Materials and methods

Study area

The White River drains a 72,520-km^2 basin covering much of northern Arkansas and southern Missouri (Figure 1). It is approximately 1,100 km in length and discharge averages 741 m^{3}s^{-1} (Schrader, Evans, & Brosset, 2006). Our sampling site lies along Scrubgrass Bayou within the Dale Bumpers White River National Wildlife Refuge (WRR), just upstream of its confluence with the Mississippi River in eastern Arkansas (34.102236, −91.061388; Figure 1). The 65,000 ha WRR includes 62,300 ha of forests (Clark & Eastridge, 2006), which makes it the largest publicly owned tract of bottomland hardwood forest in the lower Mississippi alluvial valley (Oli, Jacobson, & Leopold, 1997). Bailey (1995) places the refuge within the Lower Mississippi Riverine Forest Province, subject to a humid subtropical climate including

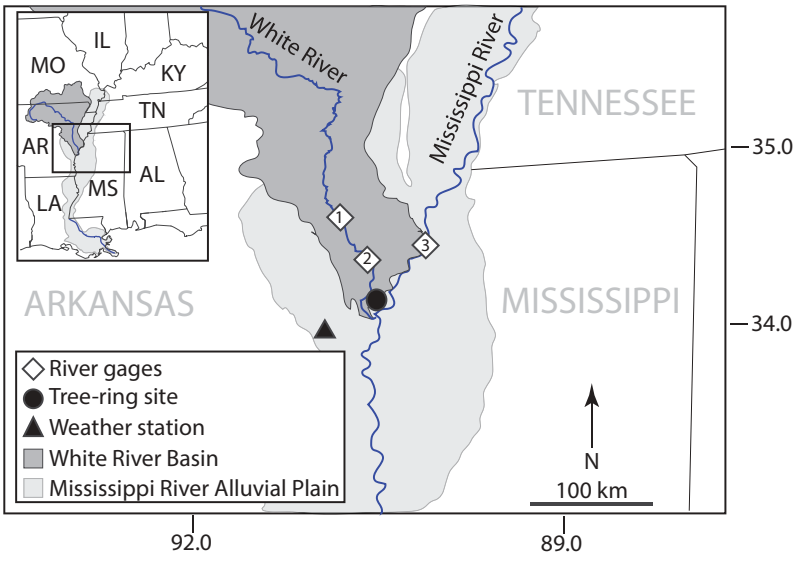

Figure 1. The tree-ring collection site at Scrubgrass Bayou (black circle); the White River gauges at St. Charles (1) and Clarendon (2), Arkansas; the Mississippi River gauge at Helena, Arkansas (3) and the Dumas, Arkansas weather station (black triangle). Also shown are the White River basin (dark grey) and Mississippi River alluvial plain (light grey).

precipitation averaging around 1,400 mm annually with an August minimum; warm winters with average temperatures 10° to 16°C and hot summers with average temperatures 21° to 27°C. Soils of the Lower Mississippi Riverine Forest Province comprise a mosaic of Inceptisols formed in alluvium, Alfisols formed in loess, and Mollisols formed in areas dominated by swampy vegetation (Bailey, 1995). Elevation ranges between 41–49 m, with the lower 75 % of the refuge experiencing prolonged inundation from winter and spring flooding (Clark & Eastridge, 2006; Oli et al., 1997). Flooding is the dominant environmental factor in bottomland forests of the lower White River (Bedinger, 1971). Prior to the development of levees along the Mississippi River in the mid-20th century, the trees along Scrubgrass Bayou would have been frequently inundated by direct overflows from both the White and Mississippi Rivers, but now flooding is normally limited to direct White River overflows and backwater flooding from the Mississippi.

Tree-ring data

We collected one-to-four increment-core samples from 23 living and cross-sections from 20 dead Overcup oak (*Q. lyrata* Walt.) trees along Scrubgrass Bayou in 2014 (Figure 1). Increment-core samples were collected using a 5-mm Swedish increment borer, as near to ground level as practical (~25 cm; St. George et al., 2002). Also included in this study are 24 increment cores from 15 living *Q. lyrata* trees from the same site previously collected by Stahle (2002). These trees were not resampled.

The samples were prepared using standard techniques (Speer, 2010) and we assigned exact annual dates to growth increments using the skeleton-plot method of cross-dating patterns of relative ring width (Stokes & Smiley, 1968). We then developed a response-index chronology

(RI) based on the proportion of analyzed trees exhibiting flood-rings compared to all trees sampled (Schroder, 1978). Only years represented by two or more trees, and those years that exceeded the boostrapped estimate of the mean frequency of flood-rings as compared to all sampled rings (10%) were included in the response-index analysis. The criteria used to identify tree rings with anatomical evidence for flood injury included abnormally small EW vessels as well as jumbled or additional ranks of EW vessels, extended EW and disorganized flame parenchyma as well as offset EW ranks (Yanosky, 1983, 1984; Astrade and Bégin, 1997; St. George & Nielsen, 2000; 2002; Wertz et al., 2013; Therrell & Bialecki, 2015; Figure 2).

We measured total ring width (RW) of each dated growth ring, and we measured the width of the first rank of earlywood vessels to develop the vessel width record (VW; Figure 3). We used the computer program COFECHA to statistically verify accurate sample dating and measuring (Holmes, 1983).

We then computed mean-value index chronologies from the RW and VW measurement series using the package dplR in the R statistical computing environment (Bunn, 2008; R Development Core Team, 2009). We also computed commonly used chronology statistics using dplR, including mean correlation within trees ($\bar{r}_{wt}$), mean correlation between trees ($\bar{r}_{bt}$), effective mean correlation ($\bar{r}_{eff}$), expressed population signal (EPS), and first-order autocorrelation (Cook & Kairiukstis, 1990).

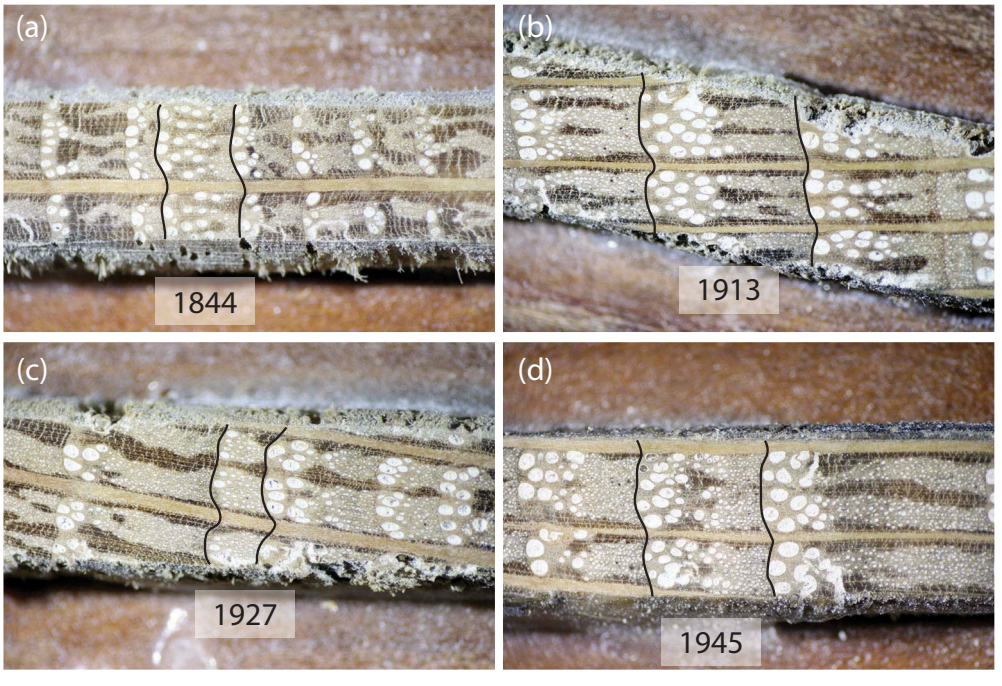

Figure 2. Microphotographs of *Quercus lyrata* annual rings (highlighted) showing various anatomical anomalies during four well documented flood years. Each example shows the diminished earlywood (EW) vessels relative to normal rings during flood years. Disorganized parenchyma are evident in (a), (c), and (d), misshapen vessels can be seen in (b) and (d) and jumbled and extended EW can be seen in (d).

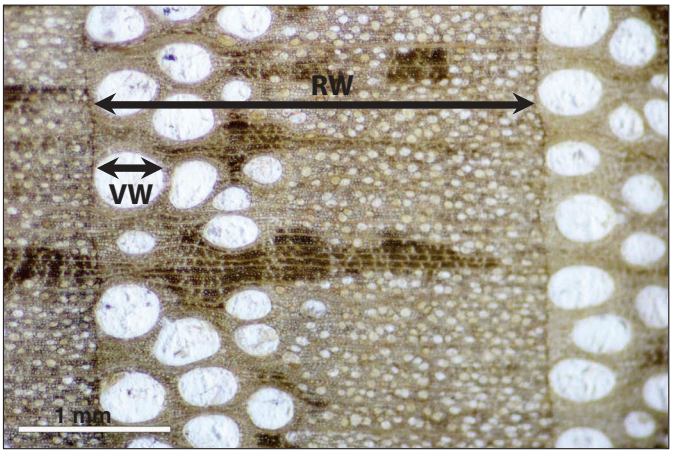

Figure 3. Measurement of *Quercus lyrata* earlywood growth increment. We used the earlywood/latewood measurement configuration of MeasureJ2X to record measurement series of the radial width of the first rank of earlywood vessels (VW) and total wing width (RW).

Climate and stage height data

To examine the sensitivity of the RI values to flood magnitude and timing, we computed Spearman's rank correlation values for the RI chronology and ranked flood stage recorded at the White River gauges at Clarendon, AR and St. Charles, AR. We also compared RI values to data from the relatively long Mississippi River gauge at Helena, AR; data for each of these three gages are available from the USACE hydrologic database (U.S. Army (USACE), 2017; Figure 1).

To determine the environmental variables to which tree growth might be responsive, we computed Pearson correlation coefficients between our RW and VW chronologies with precipitation, temperature, and river-stage height (discharge not available) for each month of the water year, from October of the year preceding growth through September of the year contemporaneous with growth. Monthly mean temperature and monthly precipitation totals are available for 64 years from 1948–2011 at the nearby weather station at Dumas, AR (Figure 1; Menne et al., 2012).

We computed monthly average river stage height from daily data measured at the most proximate river gauge at St. Charles, AR. Temporal coverage of the St. Charles gauge data is intermittent, with complete daily coverage for only 53 of the 82 calendar years in the observational period 1932–2013. Additionally, only 38 years include all annual values and also follow a year with complete annual values. We used these 38 years for the correlation analysis of St. Charles gauge mean stage heights for months October-September of the water year. Because the St. Charles hydrograph (like the Lower Mississippi River (LMR)) peaks in March through May (MAM) and most high magnitude flooding also takes place in the months of March–May, we also computed correlation coefficients for relationships of VW with mean monthly stage height for March, April and May individually and seasonalized those data into a MAM stage height mean, using all 67 available years that include complete daily coverage during those three months.

Following our comparison of VW and stage height, we reconstructed spring (MAM) mean daily White River stage heights for the period 1800–2013 using a simple linear regression of the VW chronology. We used the split-sample method of model validation to evaluate the reconstruction (e.g. Snee, 1977). The available data and predictions for our reconstruction include 67 years of MAM mean daily stage heights, computed from St. Charles gauge data for years with complete daily MAM coverage within the 1932–2013 instrumental period. For the split-sample validation we used two 33-year subsets of the 67 available years of MAM mean-stage data, one from 1932–1969, and the other from 1970–2012. We computed Pearson's *r* correlation coefficients, and reduction of error (RE) statistics for validation of each split-sample model (e.g. Cook & Kairiukstis, 1990).

Results

Visual identification of flood rings and response index

The RI chronology of flood-ring formation covers the period 1779–2013. During this time, 62 visual flood ring years were recorded by more than 10% (the theoretical background frequency) of the sampled trees (Figure 4). Rank correlations of RI values and historic crests were (r_s = 0.56, n = 9) at St. Charles (r_s = 0.48, n = 12) at Clarendon and (r_s = 0.37, n = 30) at Helena. Additionally, six of ten of the highest stage floods at St. Charles and seven of the ten largest events at Clarendon were recorded by over 30% of the sampled trees (Table 1).

During the period of overlap (1874–2013), 30 of the RI events correspond to historical stage crests at Helena, Arkansas. All but two of these floods (1957, 1973) are among the 50 highest water surface elevations (stages) out of the 190 years (137 continuous) for floods in the Helena record, with 1957 and 1973 ranked as the 18th and 5th highest crests, respectively, at St. Charles.

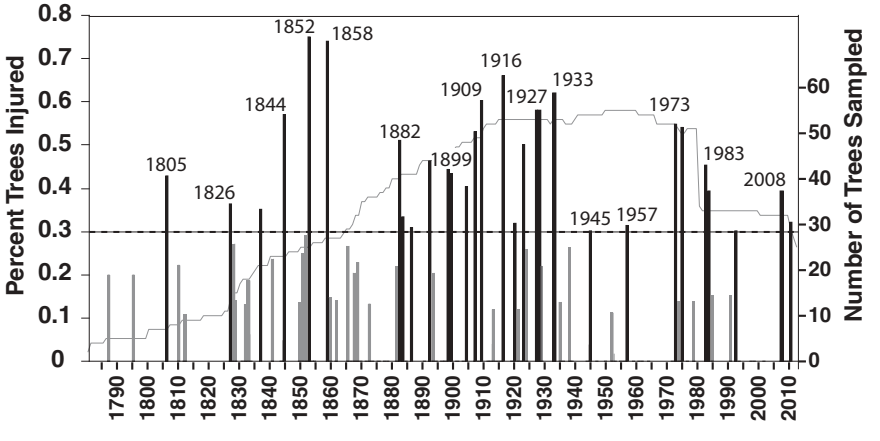

Figure 4. Flood-ring response index chronology. Vertical bars indicate the proportion of trees exhibiting anomalous anatomy in a given year. Black bars indicate years in which at least 30% of trees are affected. Sample depth (thin grey line) indicates the number of trees analyzed for year *t*. Years of notable floods in the instrumental and historical period are indicated.

Table 1. Dates of the 10 highest flood stage at the St. Charles, and Clarendon, gauges and corresponding tree-ring RI values. At St. Charles, the winter floods of 1937 and 1949 were not recorded in the RI nor was the June event in 1943. At the Clarendon gauge, 1937, 1950, and 1982 are not recorded. Again, these are winter events and 1982 is not an important flood at St. Charles.

	St. Charles				Clarendon			
	Year	Date	Stage Height (m)	RI (%)	Year	Date	Stage Height (m)	RI (%)
1	1927[a]	01-Apr	13.6	58	1927	23-Apr	13.2	58
2	1937	13-Feb	12.2	0	1945	24-Apr	11.9	30
3	2011	15-May	12.2	32	1916	07-Feb	11.7	66
4	1945	26-Apr	11.6	30	2011	10-May	11.4	32
5	1973	07-May	11.1	55	1937	28-Jan	10.9	0
6	1943	03-Jun	10.8	0	1973	03-May	10.7	55
7	1935	03-Apr	10.8	14	2008	19-Apr	10.30	39
8	2008	20-Apr	10.5	39	1975	5-Apr	10.01	54
9	1933	03-Jun	10.4	62	1982	15-Dec	10.00	0
10	1949	08-Feb	10.3	0	1950	21-Jan	9.94	06

[a] Years lacking daily stage measurements.

Chronology development and correlation analysis

There are 111 standardized index series of RW and VW (from 58 trees) included in the mean-value chronologies from 1764–2013 (Figure 5). Signal estimate statistics for both RW and VW chronologies are similar, and both RW and VW chronologies yield a good EPS, and strong ($\bar{r}_{bt}$), (Table 2). The RW chronology shows significant first-order autocorrelation (r = 0.39, $p < 0.05$), but the VW chronology does not. Correlation analysis of the RW and VW chronologies with monthly climate (n = 64 years) and stage height (n = 38 years) revealed a significant positive relationship between RW and January precipitation ($r = 0.28$, $p < 0.05$). VW shows a significant negative relationship with current-year August precipitation ($r = -0.36$, $p < 0.01$), as well as mean temperature of the previous October ($r = -0.25$, $p < 0.05$; Figure 6). The VW chronology is also significantly correlated with mean river-stage height during the December preceding growth ($r = -0.33$, $p < 0.05$) as well as March, April, May, June, July, August and September (current year) mean river-stage heights ($r = -0.50$, -0.71, -0.51, -0.43, -0.51, -0.42, -0.49; $p < 0.01$). Correlation coefficients between VW and mean daily stage for the months March, April, and May increase in significance when computed for all available years with complete coverage (n = 67) of those months ($r = -0.43$, $p < 0.01$, March; $r = -0.62$, $p < 0.01$, April; $r = -0.47$, $p < 0.01$, May). Correlation of VW with seasonalized MAM stage heights is also significant ($r = -0.62$, $p < 0.01$; Figure 6).

Stage height reconstruction

A linear-regression reconstruction of mean MAM stage height using the VW index chronology (Figure 7) reveals some degree of temporal nonstationarity in the linear relationship between vessel size and spring flooding. Split-sample model 1, calibrated on data for the 33 available years in the period 1932–1969 and validated against data for the 33 available years in the period 1970–2012, explains a significant proportion of the variance of its calibration data ($R^2 = 0.22$, $p < 0.01$). However, the fit of split-sample model 2, calibrated on the 33 available years in the period 1970–2012 and validated against the 33 years in the period 1932–1969 is better ($R^2 = 0.53$, $p < 0.01$). Split-sample model 1 is a further

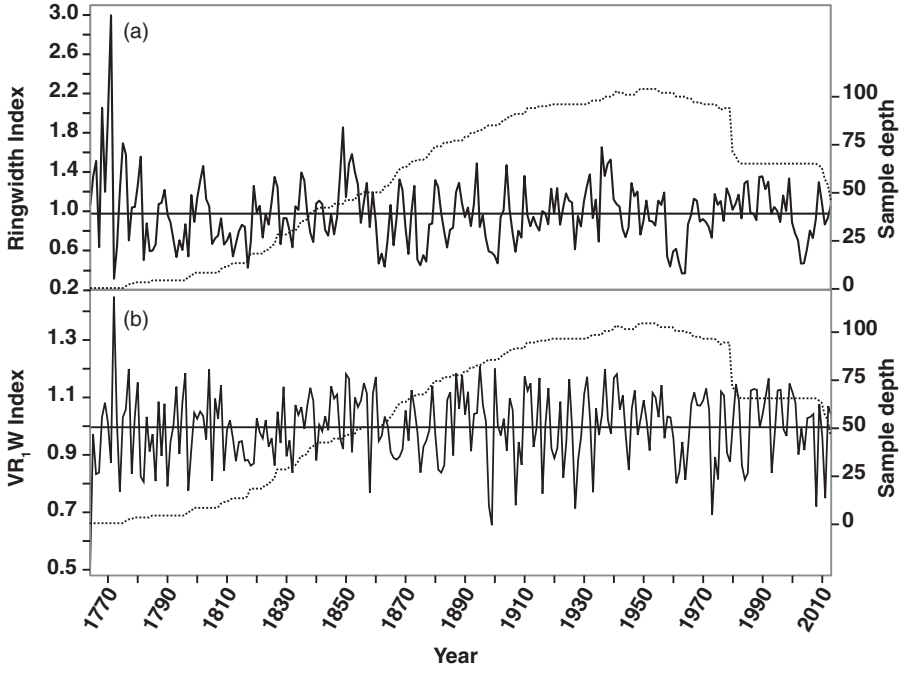

Figure 5. Ringwidth index chronology (a) and VW chronology (b). Dashed line indicates sample depth, or number of standardized measurement series contributing to chronology index value in year *t*.

Table 2. Chronology statistics for RW and VR_1W indices[1].

	n_t	$n_{\bar{t}}$	c_{eff}	$\bar{r}_{wt}$	$\bar{r}_{bt}$	$\bar{r}_{eff}$	*EPS*	r_1
RW	58	32.7	1.74	0.75	0.33	0.37	0.95	0.39
VR_1W	58	32.7	1.74	0.66	0.32	0.38	0.95	0.07

[1]Total number of trees (n_t), average number of trees contributing to each year of the chronology ($n_{\bar{t}}$), effective number of cores per tree (c_{eff}), mean correlation within trees ($\bar{r}_{wt}$), mean correlation between trees ($\bar{r}_{bt}$), effective mean correlation ($\bar{r}_{eff}$), and effective population signal (EPS) of 111 standardized series each of RW and VR_1W measurements contributing to RW and VR_1W mean-index chronologies; and first-order autocorrelation (r_1) of RW and VR_1W mean-index chronologies.

improvement (r = 0.74, RE = 0.43) over split-sample model 2 (r = 0.49, RE = 0.08), indicating that, although the strength of the linear relationship of VW to MAM stage may be weaker in the early period of the gauge record, the slope of that relationship has a better fit in the later period. Regression coefficients for the two split-sample models are not significantly different ($p > 0.05$), which indicates that calibrating a final model on the full available data is appropriate. It should be noted that cutoffs made in the late 1930s through early 1940s would likely have lowered flood levels (stages) and caused a period of rapid channel change along the LMR. Graphical analysis of both split-sample models reveals frequent over- and under-estimation of above-average MAM stage, as well as consistent over-estimation of below-average MAM stage (Figure 7). The final mean MAM stage height reconstruction extends back to 1800, as EPS values of the VW chronology indicated inadequate signal strength before 1800 (Figure 7). The final model explains 37% of the variance of the 67 years of mean MAM stage with which it was calibrated.

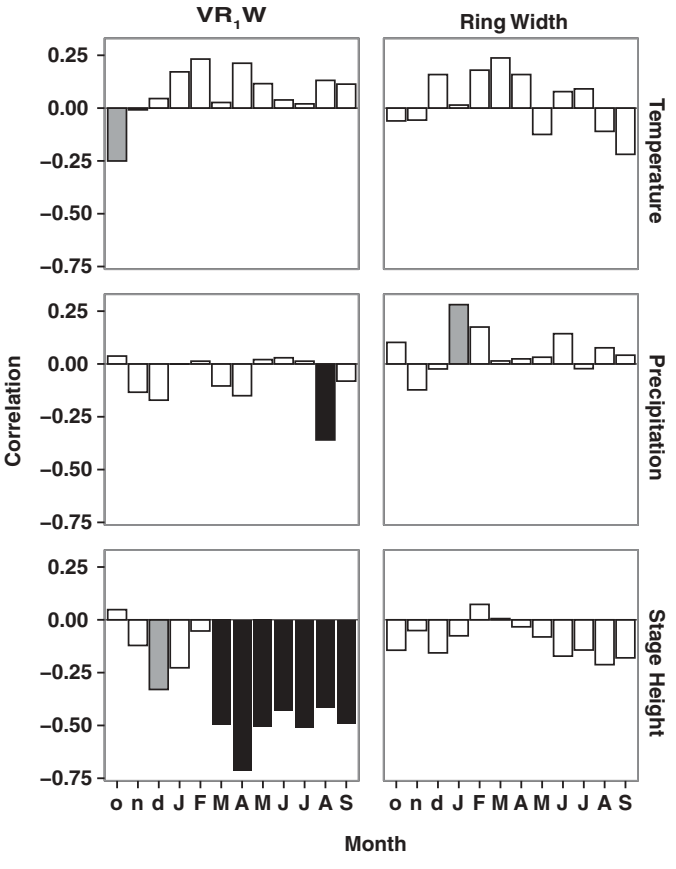

Figure 6. Monthly correlation analysis. Bar heights indicate correlation (Pearson's *r*) of index chronologies (VW, left column; RW, right column) with climate (mean temperature, upper row; precipitation, center row) and mean monthly stage height (St. Charles gauge; bottom row) for months of the water year (October of year preceding the calendar year of tree-ring growth through September of the calendar year of tree-ring growth). Gray bars indicate significance at the 0.05 level. Black bars indicate 0.01 significance level.

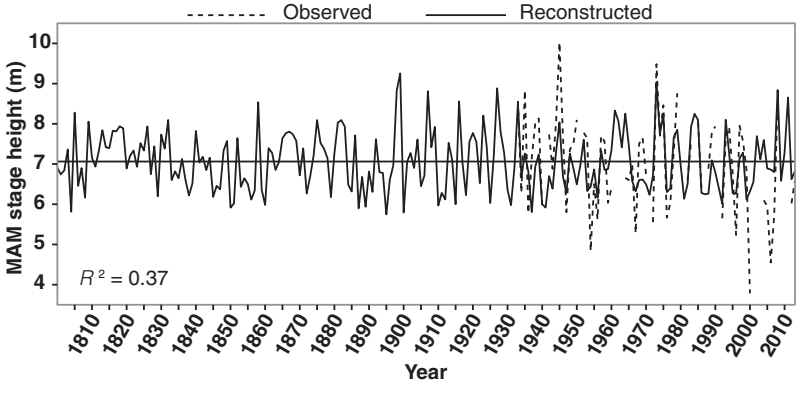

Figure 7. Observed (dashed black line; 1932–2013) and tree-ring (VW) reconstructed (solid black line; 1800–2013) MAM stage-height values for the White River gauge at St. Charles, Arkansas.

Discussion

Visual identification of flood-ring anatomical anomalies is a useful tool for exploration and analysis of tree-ring flood records. Seventy percent of the top ten historic crests in the systematic gauge record at nearby White River gauges at St. Charles and Clarendon are recorded by a large percentage (>25%) of sampled trees. Comparison to the longer Mississippi River gage at Helena Arkansas, shows that 10 of the top 20 historic crests are recorded by at least 10% of sampled trees and in most cases events that were not-recorded by trees (e.g. 1937, 1950) took place outside the growing season. Also important is the fact that all flood rings occurred in years with documented flooding, indicating that false positive results are unlikely. Prior to the instrumental period the flood ring data indicate large floods in years when flooding is documented in historical records, such as the "Great Flood" of 1844 and the well-documented 1858 flood (e.g. Humphreys & Abbot, 1867).

The RI values reflect relative magnitude of ranked historic crests better than the VW chronology, likely because the VW measurements exclude dimensions of anatomical variability that may be deemed anomalous by the type of qualitative visual analysis (e.g. shape and arrangement of vessels, porous-zone proportion of total increment, instances of interruptive fiber bands or double-earlywood "false rings," or presence of parenchyma tissue) carried out by previous researchers (e.g. St. George & Nielsen, 2000).

Our VW chronology demonstrates a novel method for efficiently quantifying inter-annual EW vessel width variability of a tree-ring sample collection. This measurement method can be performed concurrently with ring-width measurement, allowing for efficient assessment of collections for possible ecophysiological signals contained in anatomical variables. Compared to other methods for capturing EW vessel measurements, such as image analysis (Fonti, Eilmann, García- González, & von Arx, 2009), our simple method is highly efficient and our VW chronology has as strong climate signal. For example, the mean correlation between trees ($\bar{r}_{bt}$) value of 0.32 (Table 2) is comparable to or greater than many other published values (Fonti et al., 2007; García-González & Eckstein, 2003). The strong signal related to flooding contained in the Scrubgrass Bayou VW chronology supports the use of floodplain trees as proxy records of river flooding, but also highlights the limitations of relying on records produced from complex physiological processes. Chief among these limitations is the temporal window of response defined by the growing season of the responding organism.

In the case of the *Q. lyrata* trees utilized for this study, that response window apparently excludes the winter months, when important floods (though infrequent in the modern record) may occur. This limitation is exemplified by the near total absence of evidence of the 1937 flood in both the RI and VW chronologies. The VW measurement method further narrows the temporal window of quantifiable response to the period affecting formation of the first rank of EW vessels because the vessels that constitute the VW measurement likely form concurrently with or before spring bud break, leaf expansion, and twig elongation. This results in excluding anatomical variability present in the remainder of the annual growth increment. Nevertheless, the signal of spring flooding preserved in the vessel size record clearly represents a significant source of information on past environmental variability.

Both the RI and VW records indicate that floods occurred concurrent with high flows on the White River (e.g. 1927, 1945) as reconstructed by Cleaveland (2000; not shown). This coherence is perhaps somewhat surprising given that the streamflow reconstructions are for

summer (JJA) and our records indicate spring floods (MAM). However, the Cleaveland (2000) reconstruction is based on ring width growth of bald cypress (*Taxodium distichum*), which is no doubt influenced by antecedent flow conditions. Not surprisingly, years in which reconstructed high flows are known to have occurred during winter (e.g. 1950) are again not recorded as floods in this study. Although not undertaken here, it may be possible to utilize both these tree-ring datasets to develop a more comprehensive flood record for the White River.

Conclusions

Both the RI and VW records of flood response capture nearly all the major spring floods that occurred in the lower White River Basin during the systematic gauging period. Additionally, in the instrumental period there were no instances of tree-ring indicated flooding in years without associated flooding. Our new records also provide evidence of flooding in the region prior to the continuous record, including events such as those in 1805, 1826, 1844, 1852, and 1858. The "Great Flood" of 1844 and the well-known 1858 flood, were documented at other locations in the LMR in the historical record (Humphreys & Abbot, 1867), as well as by a previously developed tree-ring record of flooding in southern Missouri (Munoz et al., 2018; Therrell & Bialecki, 2015). Continued establishment of flood-ring sites and chronologies for the flood-prone bottomland forests throughout the LMR basin will no doubt reveal more information about the magnitude, frequency, and spatial extent of past floods.

Although analysis of anatomical flood response by visual examination remains important to dendrochronological paleoflood studies, VW measurement and chronology development represents a valuable method for extracting information about tree-ring environmental sensitivity that varies independently of standard tree-ring variables (e.g. ring width). This method requires negligible additional labor and no additional infrastructure compared to standard ring-width measurement and can be used for sites and species (e.g. bottomland hardwood forests, *Q. lyrata*) with relatively poor representation in dendrochronological studies of hydroclimate. Future studies should thoroughly compare the efficacy of this method to similar approaches, such as using digital image analysis, to further test the usefulness and reliability of this methodology.

Acknowledgments

We thank D.W. Stahle for access to the Scrubgrass Bayou collection, and the personnel at the Dale Bumpers White River National Wildlife Refuge for logistical support. We are also grateful for the valuable suggestions offered by two anonymous reviewers.

Disclosure statement

No potential conflict of interest was reported by the authors.

Funding

This work was supported by the U.S National Science Foundation Geography and Spatial Sciences Program [award#BSC 1359801], the University of Alabama Department of Geography, and the University of Alabama Graduate School.

ORCID

Matthew D. Therrell http://orcid.org/0000-0002-9174-6005

Data Availability

Relevant data for this study are available from Therrell, M. and Meko, M. (2019) Tree-ring dataset for flood history study in the White River, Arkansas U.S.A. *Mendeley Data, v1*. http://dx.doi.10.17632/sn22cv59rj.1. Data include earlywood vessel width and flood-ring chronologies derived from bottomland oaks (*Quercus lyrata)* growing in the White River National Wildlife Refuge. The overall site is named "Scrubgrass Bayou" (site code SGB). Data from cores collected by D. Stahle in 1980 (site code SNA; DOI https://doi.10.25921/phhr-wp20) are included in the flood ring and EW vessel width measurements. Data files include:

SGBSNA_EW_VW.crn, the earlywood vessel width chronology; SGBSNA_EW_VW_raw.text, the raw vessel width measurements; SGB_flood rings.csv, the summary percent trees injured data; SGB_individual_FRs.xlsx, the flood ring data for each tree sampled; and SGBx_secs.kml, coordinate data for the SGB collection.

References

Ashley, S. T., & Ashley, W. S. (2008). Flood fatalities in the United States. *Journal of Applied Meteorology and Climatology*, *47*, 805–818.

Astrade, L., & Bégin, Y. (1997). Tree-ring response of *Populus tremula* L. and *Quercus robur* L. to recent spring floods of the Saône River, France. *Ecoscience*, *4*, 232–239.

Bailey, R. G. (1995). *Description of ecoregions of the United States*. Washington D.C: U.S. Department of Agriculture publication 1391.

Baker, V. R. (1987). Paleoflood hydrology and extraordinary flood events. *Journal of Hydrology*, *96* (1–4), 79–99.

Ballesteros-Cánovas, J. A., Stoffel, M., St George, S., & Hirschboeck, K. (2015). A review of flood records from tree rings. *Progress in Physical Geography*, *39*(6), 794–816.

Bedinger, M. S. (1971). Forest species as indicators of flooding in the lower White River Valley, Arkansas. *US Geological Survey Professional Paper 750*. Washington, D.C.

Benito, G., Lang, M., Barriendos, M., Llasat, M. C., Francés, F., Ouarda, T., … Bobée, B. (2004). Use of systematic, palaeoflood and historical data for the improvement of flood risk estimation, review of scientific methods. *Natural Hazards*, *31*(3), 623–643.

Brázdil, R., Kundzewicz, Z. W., & Benito, G. (2006). Historical hydrology for studying flood risk in Europe. *Hydrological Sciences Journal*, *51*(5), 739–764.

Bunn, A. G. (2008). A dendrochronology program library in R (dplR). *Dendrochronologia*, *26*(2), 115–124.

Changnon, S. A., & Kunkel, K. E. (1995). Climate-related fluctuations in midwestern flood during 1921–1985. *Journal of Water Resources Planning and Management*, *121*(4), 326–334.

Clark, J. D., & Eastridge, R. (2006). Growth and sustainability of black bears at White River national wildlife refuge, Arkansas. *Journal of Wildlife Management*, *70*(4), 1094–1101.

Cleaveland, M. K. (2000). A 963-year reconstruction of summer (JJA) stream flow in the White River, Arkansas, USA, from tree-rings. *The Holocene*, *10*(1), 33–41.

Cook, E. R., & Kairiukstis, L. A. (1990). *Methods of dendrochronology: Applications in the environmental sciences*. Netherlands: Springer.

Copini, P., Den Ouden, J., Robert, E. M., Tardif, J. C., Loesberg, W. A., Goudzwaard, L., & Sass-Klaassen, U. (2016). Flood-ring formation and root development in response to experimental flooding of young Quercus robur trees. *Frontiers in Plant Science*, *7*. doi:10.3389/fpls.2016.00775

Costa, J. E. (1987). A history of paleoflood hydrology in the United States, 1800–1970. *History of Geophysics*, *3*, 49–53.

Coulthard, B., Smith, D. J., & Meko, D. M. (2016). Is worst-case scenario streamflow drought underestimated in British Columbia? A multi-century perspective for the south coast, derived from tree-rings. *Elsevier Logo*, *534*, 205–218.

Devineni, N., Lall, U., Pederson, N., & Cook, E. (2013). A tree-ring*based reconstruction of Delaware River Basin streamflow using hierarchical Bayesian regression. *Journal of Climate*, *26*(12), 4357–4374.

Downton, M., Miller, J., & Pielke, R., Jr. (2005). Reanalysis of U.S. National weather service flood loss database. *Natural Hazards Review*, *6*(1), 13–22.

England, J. F., Jr., Cohn, T. A., Faber, B. A., Stedinger, J. R., Thomas, W. O., Jr., Veilleux, A. G., … Mason, R. R. (2017). *Guidelines for determining flood flow frequency – Bulletin 17C: U.S. Geological survey techniques and methods 4–B5*. 148. doi:10.3133/tm4B5

Fonti, P., Eilmann, B., García- González, G., & von Arx, G. (2009). Expeditious building of ring-porous earlywood vessel chronologies without loosing [sic] signal information. *Trees*, *23*(3), 665–671.

Fonti, P., & García-González, I. (2004). Suitability of chestnut earlywood vessel chronologies for ecological studies. *New Phytologist*, *163*(1), 77–86.

Fonti, P., & García-González, I. (2008). Earlywood vessel size of oak as a potential proxy for spring precipitation in mesic sites. *Journal of Biogeography*, *35*(12), 2249–2257.

Fonti, P., Solomonoff, N., & García-González, I. (2007). Earlywood vessels of *Castanea sativa* record temperature before their formation. *The New Phytologist*, *173*, 562–570.

García-González, I., & Eckstein, D. (2003). Climatic signal of earlywood vessels of oak on a maritime site. *Tree Physiology*, *23*(7), 497–504.

García-González, I., & Fonti, P. (2006). Selecting earlywood vessels to maximize their environmental signal. *Tree Physiology*, *26*, 1289–1296.

Harrison, S. S., & Reid, J. R. (1967). A flood frequency graph based on tree-scar data. *Proceeding of the North Dakota Academy of Science*, *21*, 23–33.

Ho, M., Lall, U., & Cook, E. R. (2016). Can a paleo-drought record be used to reconstruct streamflow? A case-study for the Missouri River Basin. *Water Resources Research*, *52*, 5195–5212.

Ho, M., Lall, U., Sun, X., & Cook, E. R. (2017). Multiscale temporal variability and regional patterns in 555 years of conterminous U.S. streamflow. *Water Resources Research*, *53*, 3047–3066.

Holmes, R. L. (1983). Computer-assisted quality control in tree-ring dating and measurement. *Tree-Ring Bulletin*, *43*(1), 69–78.

Humphreys, A. A., & Abbot, H. L. (1867). *Report upon the physics and hydraulics of the Mississippi river* (Professional paper (United States Army Corps of Engineers), no. 13), Washington, D.C.: Government Printing Office. p. 214.

Jonkman, S. N. (2005). Global perspectives on loss of human life caused by floods. *Natural Hazards*, *34*(2), 151–175.

Kames, S., Tardif, J. C., & Bergeron, Y. (2016). Continuous earlywood vessels chronologies in floodplain ring-porous species can improve dendrohydrological reconstructions of spring high flows and flood levels. *Journal of Hydrology*, *534*, 377–389.

Klemeš, V. (1989). The improbable probabilities of extreme floods and droughts. In O. Starosolszsky & O. M. Melder (Eds.), *Hydrology of disasters* (pp. 43–51). London: James and James.

Knox, J. C. (2000). Sensitivity of modern and Holocene floods to climate change. *Quaternary Science Reviews*, *19*(1), 439–457.
López, J., Del Valle, J. I., & Giraldo, J. A. (2014). Flood-promoted vessel formation in *Prioria copaifera* trees in the Darien Gap, Colombia. *Tree Physiology*, *34*(10), 1079–1089.
Maxwell, R. S., Harley, G. L., Maxwell, J. T., Rayback, S., Pederson, N., Cook, E. R., & Rayburn, J. A. (2017). An interbasin comparison of tree-ring reconstructed streamflow in the eastern United States. *Hydrological Processes*, *31*, 2381–2394.
McCord, V. A. (1996). Fluvial process dendrogeomorphology: Reconstructions of flood events from the southwestern United States using flood-scarred trees. In J. S. Dean, et al. (Ed.), *Tree rings, environment, and humanity* (pp. 689–699). Tucson: University of Arizona.
Meko, D. M., Therrell, M. D., Baisan, C. H., & Hughes, M. K. (2001). Sacramento River flow reconstructed to AD 869 from tree rings. *Journal of the American Water Resources Association*, *37*(4), 1029–1039.
Menne, M. J., Durre, I., Korzeniewski, B., McNeal, S., Thomas, K., Yin, X., & Houston, T. G. (2012). *Global historical climatology network - Daily (GHCN-Daily), Version 3, USC00032148*. NOAA National Climatic Data Center. doi:10.7289/V5D21VHZ
Munoz, S. E., & Dee, S. G. (2017). El Niño increases the risk of lower Mississippi River flooding. *Scientific Reports*, *7*, 1772.
Munoz, S. E., Giosan, L., Therrell, M. D., Remo, J. W., Shen, Z., Sullivan, R. M., … Donnelly, J. P. (2018). Climatic control of Mississippi River flood hazard amplified by river engineering. *Nature*, *556*(7699), 95.
Oli, M. K., Jacobson, H. A., & Leopold, B. D. (1997). Denning ecology of black bears in the White River national wildlife refuge, Arkansas. *The Journal of Wildlife Management*, *61*(3), 700–706.
Pinter, N., Jemberie, A. A., Remo, J. W. F., Heine, R. A., & Ickes, B. S. (2008). Flood trends and river engineering on the Mississippi River system. *Geophysical Research Letters*, *35*(23), L23404.
R Development Core Team. (2009). *R: A language and environment for statistical computing*. ISBN 3-900051-07-0. Vienna, Austria: R Foundation for Statistical Computing. Retrieved from http://www.R-project.org
Schrader, T. P., Evans, D. A., & Brosset, T. H. (2006). *Water resources data–Arkansas, water year 2005, United States geological survey rep. USGS-WDR-AR-05-1*. Little Rock, Arkansas: Arkansas Water Science Center.
Schroder, J. (1978). Dendrogeomorphological analysis of mass movement on table cliffs plateau, Utah. *Quaternary Research*, *9*, 168–185.
Sigafoos, R. S. (1964). Botanical evidence of floods and flood-plain deposition. *US Geological Survey Professional Paper 485-A*. Washington, DC.
Snee, R. D. (1977). Validation of regression models: Methods and examples. *Technometrics*, *19*(4), 415–428.
Speer, J. H. (2010). *Fundamentals of tree-ring research*. Tucson: University of Arizona Press.
St. George, S. (2010). Tree rings as paleoflood and paleostage indicators. In M. Stoffel, et al. (Ed.), *Tree rings and natural hazards* (pp. 233–239). Netherlands: Springer.
St. George, S., & Nielsen, E. (2000). Signatures of high-magnitude 19th century floods in *Quercus macrocarpa* (Michx.) tree rings along the Red River, Manitoba, Canada. *Geology*, *28*(10), 899–902.
St. George, S., & Nielsen, E. (2002). Flood ring evidence and its application to paleoflood hydrology of the Red River and assiniboine river in Manitoba. *Geographie physique et Quaternaire*, *56* (2–3), 181–190.
St. George, S., & Nielsen, E. (2003). Palaeoflood records for the Red River, Manitoba, Canada derived from anatomical tree-ring signatures. *Holocene*, *13*(4), 547–555.
St. George, S., Nielsen, E., Conciatori, F., & Tardif, J. (2002). Trends in *Quercus macrocarpa* vessel areas and their implications for tree-ring paleoflood studies. *Tree-Ring Research*, *59*(1–2), 3–10.
Stahle, D.W. (2002, Apr 26): NOAA/WDS Paleoclimatology - Stahle - Sugarberry - QULY - ITRDB AR021. NOAA National Centers for Environmental Information. [accessed 2015 Jan 26]. Retrieved from https://doi.org/10.25921/phhr-wp20

Stedinger, J. R., & Griffis, V. W. (2008). Flood frequency analysis in the United States: Time to update. *Journal of Hydrologic Engineering*, *13*(4), 199–204.

Stokes, M. A., & Smiley, T. L. (1968). *An introduction to tree-ring dating*. Chicago, Ill: Univ. of Chicago Press.

Tardif, J. C., Kames, S., & Bergeron, Y. (2010). Spring water levels reconstructed from ice-scarred trees and cross-sectional area of the earlywood vessels in tree-rings from eastern boreal Canada M. Stoffel. In M. Bollschweiler, D. R. Butler, & B. H. Luckman (Eds.), *Tree-rings and natural hazards: A state-of-art. Advances in global change research* (Vol. 41, pp. 257–261). Springer.

Therrell, M. D., & Bialecki, M. B. (2015). A multi-century tree-ring record of spring flooding on the Mississippi River. *Journal of Hydrology*, *529*, 490–498.

U.S. Army (USACE). (2017). RiverGauges.com, water levels of rivers and lakes. Retrieved from www.rivergauges.com

Wertz, E. L., St. George, S., & Zeleznik, J. D. (2013). Vessel anomalies in *Quercus macrocarpa* tree rings associated with recent floods along the Red River of the North, United States. *Water Resources Research*, *49*(1), 630–634.

Woodcock, D. W. (1989). Climate sensitivity of wood-anatomical features in a ring-porous oak (*Quercus macrocarpa*). *Canadian Journal of Forest Research. Journal Canadien De La Recherche Forestiere*, *19*, 639–644.

Woodhouse, C. A., & Lukas, J. J. (2006). Multi-century tree-ring reconstructions of Colorado streamflow for water resource planning. *Climatic Change*, *78*(2–4), 293–315.

Yanosky, T. M. (1983). Evidence of floods on the Potomac River from anatomical abnormalities in the wood of flood-plain trees. *U.S. Geol. Surv. Prof. Pap. 1296*. Washington DC.

Yanosky, T. M. (1984). Documentation of high summer flows on the Potomac River from the wood anatomy of ash trees. *Water Resources Bulletin*, *20*, 241–250.

Yanosky, T. M., & Jarrett, R. D. (2002). Dendrochronologic evidence for the frequency and magnitude of paleofloods. In P. K. House, et al., (Ed.), *Ancient floods, modern hazards* (pp. 77–89). Washington, DC: American Geophysical Union. doi:10.1029/WS005p0077